Adsorption Behavior of Cr(VI) from Aqueous Solutions by Microwave Modified Porous Larch Tannin Resin

Zhanhua Huang,* Bin Zhang, and Guizhen Fang

Larch tannin resin (LTNA) was prepared by a microwave modified cross-linking reaction. The adsorption of chromium(VI) from an aqueous solution by LTNA was studied using batch adsorption experiments. LTNA has a large number of pores, the size of which are about 250 nm. After adsorption, the internal structure of the LTNA resin assumed an obvious three-dimensional network. The adsorption of Cr(VI) on LTNA was investigated as a function of pH, dose of adsorbent, and adsorption time. The results indicated that the removal of Cr(VI) was pH-dependent. The optimum adsorption was observed at pH 1.0, and the maximum adsorption capacity was 9.134 mg/g. The Cr(VI) adsorption by the LTNA gel obeyed the Langmuir adsorption isotherm. The kinetic processes of Cr(VI) adsorption onto LTNA could be acceptably explained by the pseudo-second order kinetic rate model. Thermodynamic parameters revealed the spontaneity and exothermic nature of adsorption. Desorption of adsorbed Cr(VI) was successfully realized with a 0.1 M NaOH solution.

Keywords: Larch tannin; Mesoporous; Adsorption; Cr(VI); Microwave irradiation

Contact information: Key laboratory of Bio-based Material Science and Technology of Ministry of Education, Northeast Forestry University, Harbin 150040, China;
** Corresponding author: huangzh1975@163.com*

INTRODUCTION

Chromium is a heavy metal widely present in effluents from industries such as leather, dyeing, electroplating, mining, and photography (Owlad *et al.* 2010). There are two major oxidation states of soluble chromium species Cr(III) and Cr(VI). Cr(III) is one of the necessary trace elements in the human body and has low solubility and mobility in soils and aqueous environments (Albadarin *et al.* 2012). However, Cr(VI) is a highly toxic material and exists as extremely soluble chromate ions ($HCrO^{4-}$ or $Cr_2O_7^{2-}$), which can be transferred freely in aqueous environments (Mitra *et al.* 2011). Cr(VI) can accumulate in the food chain and may causes diseases, such as cancer in the digestive tract and lungs, perforation of the nasal septum, skin dermatitis, bronchitis, severe diarrhea, and hemorrhaging, *etc.* (Marjanovic *et al.* 2011).

The various methods of chromium removal include chemical precipitation, adsorption, reverse osmosis, membrane systems, electrolytic process, and ion exchange (Hu *et al.* 2011). Among these methods, adsorption is one of the most economically favorable and technically easy (Karthikeyan *et al.* 2005). In recent years, using adsorption to deal with heavy metal has become a hot topic. Conventional adsorbents that have been used to remove Cr(VI) from industrial wastewaters include activated carbon (Liu *et al.* 2010a), metal oxide adsorbents, non-metal oxide adsorbents, organic absorbent materials, and biomass adsorbent materials (chitosan, tannin, cellulose) (Miretzky and Cirelli 2010). However, many absorbents, apart from being expensive, have

disadvantages such as lower adsorption capacity and difficult regeneration (Singha and Kumar 2011). Therefore, considerable attention has been focused on the removal of Cr(VI) from aqueous solutions using biomaterial adsorbents derived from low-cost materials. The materials tested as Cr(VI) adsorbents include straw (Ahalya *et al.* 2005), sawdust (Gupta and Babu 2009), hyacinth roots, neem leaves, coconut shell (Singha and Kumar Das 2011), fruit shell (Anandkumar and Mandal 2009), pine needles (Uysal and Ar 2007), jute fiber (Kumara *et al.* 2008), algae (Gupta *et al.* 2001), walnut hull (Wang *et al.* 2009), *Trapa natans* husk (Liu *et al.* 2010b), rice husk (Guo *et al.* 2002), and bark (Huang *et al.* 2010).

Larch tannin was extracted from wasted barks of *Larix gmelinii* (Rupr.). The condensed tannin (Ayhan Sengil and Özaca 2009) with resorcinol A-rings and catechol B-rings is shown in Fig. 1. The adjacent hydroxyl groups on the larch tannin exhibiting specific affinity to metal ions can probably be used as alternative and effective adsorbents for the removal of metal ions (Oo *et al.* 2009). However, there is limited data available on Cr(VI) removal using larch tannin.

The purpose of this investigation is to obtain an understanding of the equilibrium adsorption of Cr(VI) on LTNA by studying the influence of different experimental parameters on the adsorption process. Moreover, experimental kinetic data will be investigated using the pseudo-first order, pseudo-second order, intra-particle diffusion, and Elovich kinetic equations.

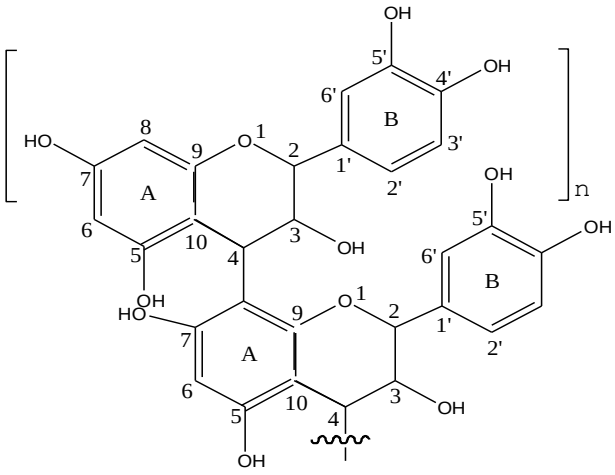

Fig. 1. The flavonoid unit in larch tannin (n ≤ 9)

EXPERIMENTAL

Materials

Larch tannin (LT) was obtained from the bark of *Larix gmelini* Rupr. by extraction with a 65 °C water solution, followed by spray drying (Oo *et al.* 2009). The tannin content of the extract was 78.1%, determined by the hide powder method, a national standard method of China (code: GB2615-81). The stock solution of $K_2Cr_2O_7$ (0.2 to 1.0 mg/L) was prepared by dissolving $K_2Cr_2O_7$ in deionized water. Dilute solutions of HNO_3 and NaOH were used for adjusting the initial pH of solutions.

Preparation of Larch Tannin/NMBA/AA (LTNA) Resin

Fifteen grams of larch tannin powder were dissolved in 21 mL 0.1 mol/L NaOH solution, then placed into a 500 mL 4-necked round-bottom flask, and 50 mL of cyclohexane was added. The mixture was stirred under a nitrogen atmosphere in a microwave synthesizer. Aqueous solutions of 8 g acrylic acid (AA), 4 g N, N-methylene-bis-acrylamide (NMBA), and 0.385 g $K_2S_2O_8$ were poured into two drop funnels under constant pressure to provide the monomer and initiator solution systems, respectively. The monomer and initiator solutions were added to the reactor at 40 °C, and the exposure time was 0.5 h under microwave power. When the cross-linking chemical reaction was finished, the temperature was maintained at 60 °C for 60 min. The larch tannin gel was dried under vacuum at 40 °C for 24 h, and the tannin gel obtained was crushed and sieved to produce 40 μm particles. And at the same react condition, LTNA was synthesized by regular chemistry synthesizer. The Brunauer-Emmett-Teller (BET) surface area was measured from N_2 adsorption isotherms at 77 K with an automatic adsorption apparatus (ASAP 2020). The specific surface areas of the larch tannin resin are given in Table 1.

Table 1. Main Properties of LTNA Resin

Adsorbent	LTNA (microwave)	LTNA (regular synthesizer)
BET surface area (m^2g^{-1})	0.2928	0.1048
T-plot micropore area (m^2g^{-1})	0.7365	0.2083
Micropore volume (cm^3g^{-1})	0.000307	0.000094
Average pore diameter (nm)	35 to 400	60 to 750

Characterizations

Scanning electron microscope (SEM) images were taken with an FEI QUANTA 200 microscope. The hydrogels that were swollen to equilibrium in Cr(VI) concentrations of 1.0 mg/L at 37 °C for 24 h were frozen and immediately snapped. The fracture surface (cross-section) of the hydrogel was observed and photographed. Fourier transform-infrared (FTIR) spectra of the initial LT and LTNA resin were recorded with a MAGNA 560 FTIR spectrometer from Thermo Nicolet Corporation. A pressed pellet was prepared by grinding the sample powder with IR grade KBr in an agate mortar. The wavelength scan range was 4000 to 400 cm^{-1} with a resolution of 4 cm^{-1} and an interval of 1.0 cm^{-1}.

Adsorption Experiments

$K_2Cr_2O_7$ was dissolved in deionized water and then diluted to the required concentration after the pH was adjusted using HNO_3 or NaOH. A certain amount of the prepared adsorbent was added to solutions containing various concentrations of Cr(VI) ions. The ions were allowed to adsorb at room temperature for 4 h before the solution was filtered. The concentration of Cr(VI) ions in the filtrate was measured by an atomic adsorption spectrophotometer. The adsorption capacity Q and removal rate A (Huang *et al.* 2012) were calculated as follows,

$$Q = \frac{C_0 V_0 - C_e V_e}{m} \quad (1)$$

$$A = \frac{C_0V_0 - C_eV_e}{C_0V_0} \times 100\% \quad (2)$$

where C_0 and C_e are the initial and equilibrium concentrations of Cr(VI), respectively, V_0 and V_e are the initial and equilibrium volumes of the solution, respectively, and m is the mass of the LTNA resin used.

To determine the adsorption kinetics and adsorption isotherms, 100 mL of the Cr(VI) solution (equivalent to 0.2 mg/L, 0.4 mg/L, 0.6 mg/L, 0.8 mg/L, or 1.0 mg/L) was added to 0.2 g of the LTNA resin. The temperature was maintained at 25 °C, and the solution was shaken for 120 min. At various intervals, the adsorbent and the solution were separated by filtration and the adsorbent was weighed. The solution phase was diluted, and the Cr(VI) concentration was measured. Effects of the amount of adsorbent, pH, and adsorption time on the adsorption capacity were systematically investigated.

RESULTS AND DISCUSSION

Morphological Investigation

Figure 2 shows SEM images of LTNA resin incubated in different liquid media.

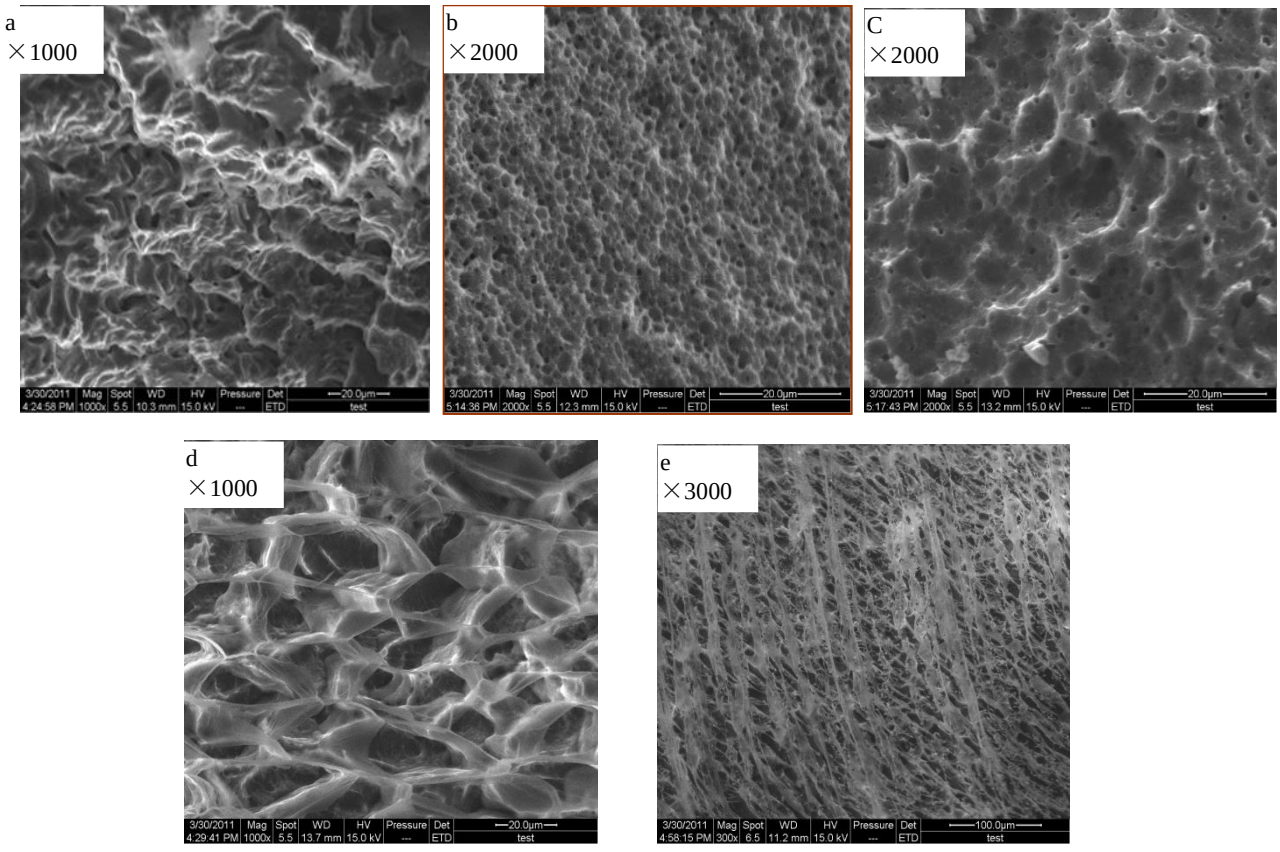

Fig. 2. SEM images of (a) Tannin resin by regular synthesizer, (b, c) LTNA resin by microwave modified, (c) in distilled water, (d) in 1.0 mol/L Cr(VI) solution

An SEM image of the dry resin prepared by regular synthesizer is shown Fig. 2(a), and SEM images of the LTNA dry resin prepared with microwave modification are shown in Figs. 2(b) and (c). It can be seen in Fig. 2(c) that the resin produced through graft copolymerization of LT with AA and NMBA in microwave synthesizer had a larger number of pores relative to the product (Fig. 2(a)) prepared by regular synthesizer. The size of the pores was about 250 nm, which provided a large adsorption surface area and improved exchange and adsorption processes. The SEM images of the LTNA resin in distilled water and in Cr(VI) solution are shown in Figs. 2(d) and 2(e), respectively. After adsorption, the internal structure of the LTNA resin assumed an obvious three-dimensional network. The network size was smaller in Cr(VI) solution than in distilled water. This revealed that competitive adsorption in LTNA resin between the Cr(VI) and H_2O occurred.

Fourier Transform Infrared Spectroscopy

Fourier transform infrared (FTIR) spectra of LT and LTNA are shown in Fig. 3. The peak for the stretching vibration adsorption of –OH was around 3400 cm^{-1}, the stretching vibration peak for C-H was located at 2900 cm^{-1}, while the stretching vibration peak for the carboxylic acid -C=O was 1600 to 1700 cm^{-1}, and the bending vibration peak for C-H was near 1450 cm^{-1}.

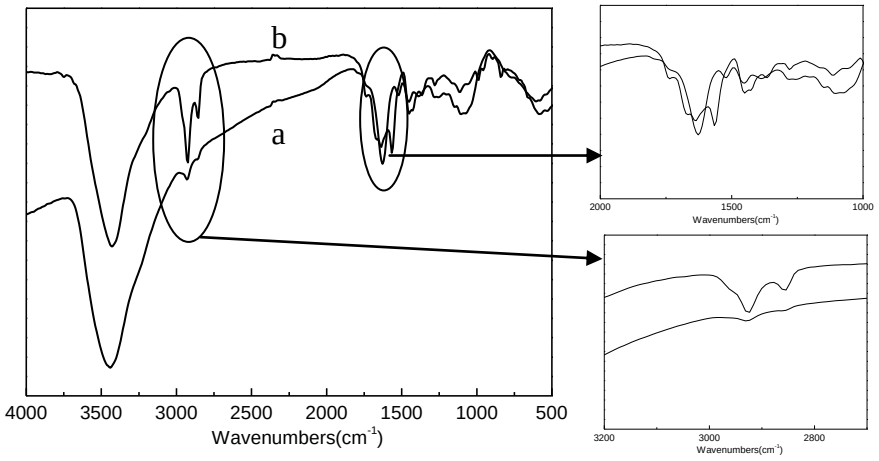

Fig. 3. FTIR spectra of (a) LT and (b) LTNA resin

Comparing the FTIR spectra for LT and LTNA, -CH_2 stretching vibrations at 2924 cm^{-1} and 2848 cm^{-1} increased significantly in LTNA, possibly due to the formation of -CH_2 in the polymerization process during the introduction of AA and NMBA monomers. The strong, overlapping peaks that occurred at 1745 cm^{-1} can be attributed to the -C=O stretching vibration peaks in acid amides and carboxylic acids. The strong stretching vibration peak at 1530 cm^{-1} in the LTNA was the N-H adsorption peak in an amide group (Kim and Kim 2003). The asymmetric stretching vibration of the sodium carbonyl group of –COONa in sodium polyacrylate is seen in the peak at 1480 cm^{-1} in the LTNA. Based on these results, it can be concluded that carboxyl and amide groups had been introduced to the LTNA, and the lack of a characteristic -C=C adsorption peak indicates that a polymerization reaction had occurred between LT, AA, and NMBA. The

vibration peaks at 1616 cm^{-1} and 1518 cm^{-1} in the LT can be attributed to the skeleton of benzene, but in LTNA, they were covered by the N-H adsorption peak at 1530 cm^{-1} and the -C=O stretching vibration peaks at 1745 cm^{-1}, thus becoming a peak having the shape of steamed bread (Oo *et al.* 2009). Based on these results, it can be concluded that -CH_2, -C=O, N-H, -COONa, and benzene have been introduced to the LTNA product, indicating that a polymerization reaction had occurred.

Adsorption Studies

Effects of adsorbent dosage

As shown in Fig. 4(a), the removal rate of Cr(VI) was highest at the LTNA dosage of 0.10 g. The maximum removal rate of Cr(VI) was 69.08% and the adsorption capacity was 337.28 μg/g. The removal rate showed a smooth upward trend with increasing LTNA dosage. In contrast, the adsorption capacity gradually decreased with increasing LTNA dosage. The decrease in adsorption capacity is attributable to the splitting effect of the concentration gradient between sorbate and sorbent with increased LTNA dosage, causing a decrease in the amount of Cr(VI) adsorbed onto a unit weight of LTNA (Uysal and Ar 2007). Meanwhile, the added adsorbent provided excessive active groups beyond the capacity to be accepted by Cr(VI) ions. In addition, due to competition between water and Cr(VI) ions for active groups on the adsorbent, an increase in water adsorption capacity would result in a decrease in the adsorption of Cr(VI) ions.

Effect of pH on Cr(VI) uptake by LTNA

Fig. 4(b) shows that the removal rate and the Cr(VI) adsorption capacity of LTNA decreased from 489.57 μg/g to 133.82 μg/g when the medium pH was increased from 1.0 to 13.0. As seen from this figure, the adsorption of Cr(VI) onto LTNA was strongly pH-dependent. The optimum pH (1.0) was observed with a 98.8% Cr(VI) removal rate and the maximum the Cr(VI) adsorption capacity. There was a sharp decrease in the removal when the solution's pH was raised from 2.0 to 6.0. Similar results were reported by other researchers (Guo *et al.* 2002). The decrease in the adsorption with increasing solution pH may be described as the decrease in electrostatic force of attraction between the adsorbent and the adsorbate. The FTIR (Fig. 3) of LTNA shows that there are several functional groups: amine, carboxyl, hydroxyl groups, *etc*. These functional groups are responsible for Cr(VI) binding onto the surface of LTNA.

At solution pH values between 2.0 and 6.0, the ionic form of Cr(VI) is clearly pH-dependent. $Cr_2O_7^{2-}$ is predominant in basic solutions, while $Cr_2O_7^{2-}$, $HCrO_4^-$, and CrO_4^{2-} are predominant at pH 2.0-6.0 (Benhammou *et al.* 2007; Tazrouti and Amrani 2009). At lower pH (pH < 2.0), the principal species are $Cr_4O_{13}^{2-}$ and $Cr_3O_{10}^{2-}$ (Miretzky and Cirelli 2010). These anionic species can be adsorbed to the protonated active sites of the bio-sorbent. Instead of Cr(VI), Cr(III) may also be present in the acidic solution. The reduction of Cr(VI) into Cr(III) could occur during adsorption of Cr(VI) on a network of the tannin gel particles (Nakano *et al*. 2001). However, the amount of Cr(III) present under different pH conditions was not determined. This issue would be considered in future studies.

Within the pH range of 1.0 to 2.0, Cr(VI) existed in the form of H_2CrO_4, and protonation of the amino groups of LTNA enhanced the Cr(VI) ion adsorption capacity of LTNA. Via the positively charged ligands on the surface of LTNA, under strongly acidic conditions (pH <2.0), an electrostatic effect was produced by the electron-donor groups of LTNA contacting with Cr(VI), subsequently resulting in the binding of Cr(VI)

to the LTNA. In solution, the dominant form of Cr(VI) at pH 1.0 to 2.0 is H_2CrO_4, and at pH 3.0 it is $HCrO_4^-$. In increasing pH, the acid chromate ion species ($HCrO_4^-$) shifts to other forms (Huang *et al.* 2010). In an aqueous solution below pH 6.0, the amino groups of LTNA would be in a protonated cationic form to a higher extent, which would result in a stronger attraction for negatively charged ions. Additionally, electrostatic interaction occurred between the sorbent and $HCrO_4^-$ ions, resulting in extensive chromium removal (Aydın and Aksoy 2009).

The fact that a higher pH decreased the adsorption capacity may be explained by the dual competition of both anions (CrO_4^{2-} and OH^-) to be adsorbed on the surface of the adsorbent, of which OH^- predominates (Karthikeyan *et al.* 2005). As a result, pH 1.0 was selected as the optimum pH value for the Cr(VI) solution in the subsequent adsorption experiments.

Effect of adsorption time

The experiments were conducted at room temperature, with 0.1 g LTNA and Cr(VI) concentrations of 0.2 mg/L, 0.4 mg/L, 0.6 mg/L, 0.8 mg/L, and 1.0 mg/L. The adsorption capacities of LTNA for Cr(VI) after various adsorption durations are shown in Fig. 4(c). The Cr(VI) adsorption capacity of LTNA at different concentrations increased with an increase of contact time, and equilibrium was reached in 1.5 h. The initial rate was rapid; about 70-75% uptake of Cr(VI) was achieved during the first 30 min and the remaining removal occurred in the following 100 min. There was no significant influence of contact time on the adsorption efficiency after 1.5 h. The adsorption equilibrium time of Cr(VI) by LTNA was shorter than CMCF and CMCN (Sankararamakrishnan *et al.* 2006). Based on the adsorption curve, the adsorption of Cr(VI) onto LTNA can be divided into two phases: the rapid adsorption stage (the adsorption of Cr(VI) onto the outer surface of LTNA) and the slow adsorption stage (progressive adsorption). Because there were a large number of active sites on the surface of the LTNA resin, the concentration differences caused a fast mass transfer during the initial phase and the Cr(VI) was easily absorbed by the resin (Ayhan Sengil and Özacar 2009). With the increase in initial Cr(VI) concentration from 0.2 to 1.0 mg/L, the adsorption capacity decreased from 913.3 µg/g to 44.5 µg/g, indicating that the adsorption capacity is highly dependent on initial concentration. For a fixed adsorbent dose, the total available sites were limited so that a decrease in percentage adsorption corresponding to an increase in initial solution concentration occurred. In other words, at lower Cr(VI) concentrations, adsorption equilibrium was achieved faster and the equilibrium time extended with an increase in the Cr(VI) concentration. When the contact time was longer than the equilibrium time, the concentration of Cr(VI) in the residual solution remained unchanged. The result implies no change of the adsorption capacity.

Isotherm studies

The adsorption modeling of isotherm data is important for predicting and comparing the adsorption performance. The equilibrium data for Cr(VI) adsorption at 25 ^oC were evaluated using Langmuir and Freundlich isotherm models.

The Langmuir isotherm model assumes that the adsorbate molecules form an adsorbed layer with one molecule in thickness and that all sites are equal, resulting in equal energies and enthalpies of adsorption. The Langmuir isotherm model (Langmuir 1918) is given by,

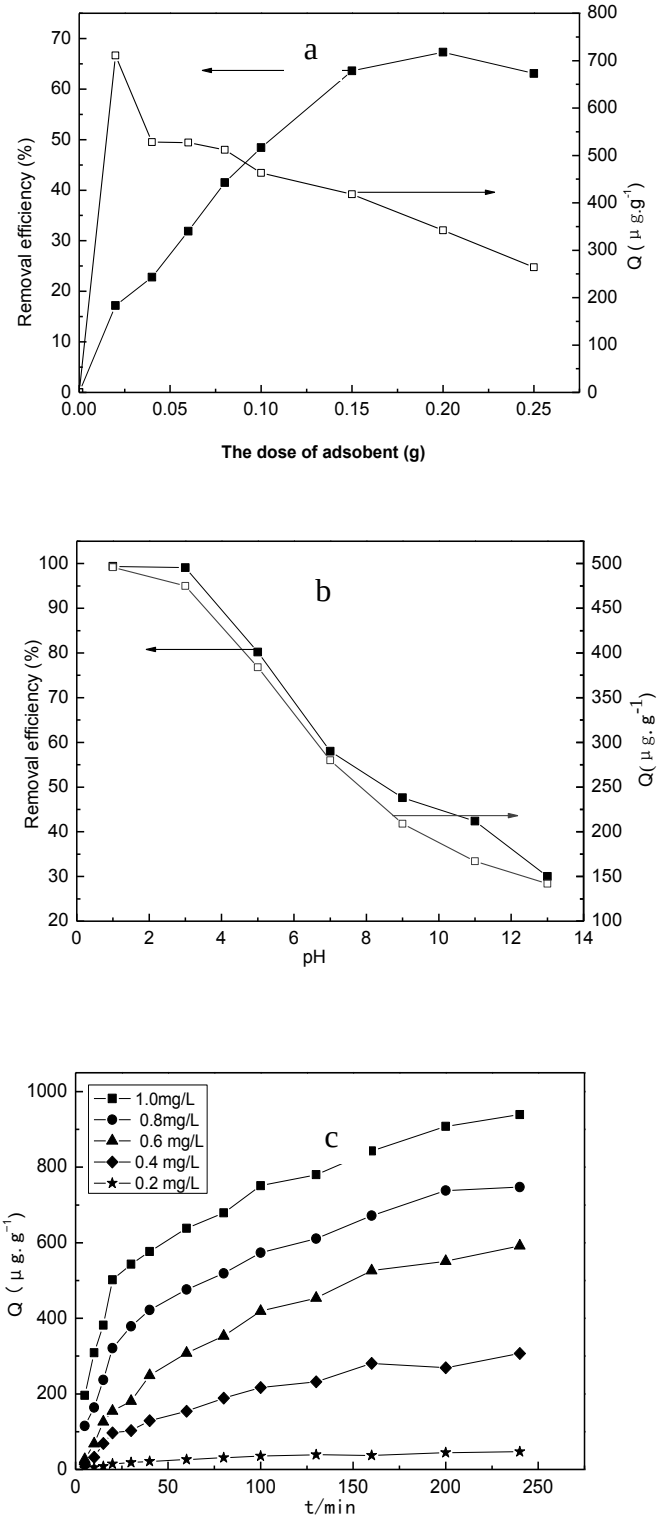

Fig. 4. Effect of (a) the adsorbent dosage, (b) initial pH, and (c) contact time on the Cr(VI) adsorption capacity of LTNA

$$q_e = \frac{q_{\max} K_L C_e}{1 + K_L C_e} \quad (3)$$

where q_e is the adsorbed amount at equilibrium (mg/g), C_e is the equilibrium concentration of the adsorbate (mg/L), q_{max} is the Langmuir monolayer sorption capacity (mg/g), and K_L is the Langmuir equilibrium constant (L/mg) related to the energy of adsorption and affinity of the adsorbent.

The Freundlich isotherm model is derived by assuming a heterogeneous surface with a non-uniform distribution of heat of adsorption over the surface. The Freundlich isotherm model (Freundlich 1906) is given by,

$$\log q_e = \log K_F + \frac{1}{n_F} \log C_e \quad (4)$$

where K_F (mg/g) and n_F (g/L) are the Freundlich constants related to the adsorption capacity and the intensity of adsorption, respectively.

The results of the isotherm constants and the coefficients of determination for the isotherm plots of Cr(VI) are given in Table 2. The Langmuir adsorption capacity, q_{max}, was determined to be 9.134 mg/g. The adsorption capacity of the treated larch bark was 6.8 mg/g (Aoyama and Tsuda 2001). However, larch tannin has a large molecular weight and the activated hydroxyl content was limited. So, the Cr(VI) adsorption capacity of larch tannin modified material is lower than Mimosa tannin gel (Nakano *et al*. 2001) and Persimmon tannin gel (Nakajima and Baba 2004). The relatively lower monolayer adsorption capacity of LTNA compared to the reported larch tannin adsorbent (Chand *et al*. 2009) is due to the presence of active acidic functional groups and hydroxy groups on LTNA. The adsorption capacity value K_F and n_F for Cr(VI) obtained from Freundlich model were evaluated to be 11.122mg/g and 1.105g/L, respectively. The value of n_F was determined as 1.105. The fact that this value lies in the range 1.0 to 10.0 indicates the favorable adsorption of Cr(VI) onto LTNA. Therefore, the adsorption mechanism of Cr(VI) to LTNA takes place through an ion exchange process (Homagai *et al*. 2010).

Table 2. Adsorption Isotherm Constants of the Langmuir and Freundlich Models for Cr(VI) Adsorbed to LTNA

Model	Coefficient	Cr(VI)
Langmuir	q_{max}(mg/g)	9.134
	K_L(L/mg)	2.091
	R^2	0.988
Freundlich	K_F (mg/g)	11.122
	n_F	1.105
	R^2	0.996

Adsorption Kinetics

To analyze the mechanism of adsorption and its potential rate-controlling steps in the adsorption process, kinetic models were exploited. Several kinetic models, such as pseudo-first order, pseudo-second order, the Elovich equation, and the intra-particle

diffusion equation were applied to determine adsorption mechanisms. Equations of the four kinetic models (Hu *et al.* 2011) were expressed as follows:

The pseudo-first-order rate equation is given as,

$$\log(Q_{e,1} - Q_t) = \log Q_{e,1} - \frac{K_1}{2.303} t \quad (3)$$

where Q_t and Q_e,1 represent the amount of adsorbed Cr(VI) on the adsorbent at time t and at equilibrium, respectively (mg.g^{-1}), and K_1 is the adsorption equilibrium rate constant (min^{-1}).

The linearized form of the pseudo-first order model for the adsorption of Cr(VI) ions onto LTNA at various initial concentrations is given in Fig. 5(a). The calculated results of the pseudo-first order rate equation are listed in Table 2. The equilibrium adsorption capacity of LTNA increased with increasing Cr(VI) concentration. The R^2 values for the pseudo-first order kinetic equations fitted for different Cr(VI) concentrations were all greater than 0.65 with no regular variation. Therefore, the adsorption of Cr(VI) onto LTNA does not follow the pseudo-first order rate equation (Hu *et al.* 2011). One suggestion for the differences in experimental and theoretical Q_e values is that there is a time lag, possibly due to a boundary layer or external resistance at the beginning of the adsorption, however, this time lag is difficult to quantify. As a result, it is necessary to use a trial and error method in order to obtain the equilibrium uptake.

The pseudo-second order kinetic equation (Hu *et al.* 2011) is shown as follows,

$$\frac{t}{Q_t} = \frac{1}{K_2 Q_{e,2}^{\ 2}} + \frac{1}{Q_{e,2}} t \quad (4)$$

where K_2 is the equilibrium constant of the pseudo-second order equation (g mg^{-1} min^{-1}), and Q_e is the adsorption capacity calculated by the pseudo-second order kinetic model (mg g^{-1}).

The linearized form of the pseudo-second order kinetic model is given in Fig. 5(b). The best-fit values of model parameters and coefficients of determination for the equations are listed in Table 2. The R^2 values, depending on the concentration of Cr(VI), ranged from 0.92 to 0.98. The calculated Q_e values agreed very well with the experimental data, indicating that the adsorption process was in line with a pseudo-second order kinetic model. The experimental results support the assumption included in the model that the rate-limiting step in adsorption of heavy metals is chemisorptions involving valence forces through the sharing or exchange of electrons between metal ions and adsorbent. Some studies on the kinetics of Cr(VI) adsorption onto various adsorbents have also reported higher correlations with the pseudo-second order kinetic model (Sankararamakrishnan *et al.* 2006).

The pseudo-first order and pseudo-second order kinetic models described above cannot determine the diffusion mechanism of Cr(VI) onto LTNA resin because the adsorption process on a porous adsorbent is usually a multi-step process. Therefore, to investigate the mechanism of the adsorption of Cr(VI) onto LTNA, the experimental data were tested against the intra-particle diffusion equation and the Elovich equation to identify the mechanism in the adsorption process.

The intra-particle diffusion equation (Huang *et al.* 2012) is based on the model proposed by Weber and Morris, which is as follows,

$$O_t = K_{\text{int}} t^{1/2} + C \quad (5)$$

where K_{int} is the constant for the particle diffusion rate (mg g^{-1} $min^{-1/2}$) and C of adsorption constant is the intercept. There are three consecutive steps in the adsorption of an adsorbate by a porous sorbent: (i) mass transfer across the external boundary layer of liquid surrounding the outside of the adsorbent particle, (ii) adsorption at a site on the surface, where the energy will depend on the binding chemical or physical process (this step is often assumed to be very rapid), and (iii) diffusion of the adsorbate molecules to an adsorption site either by a pore diffusion process by the liquid-filled pores or through a solid surface diffusion mechanism (Hu *et al.* 2011).

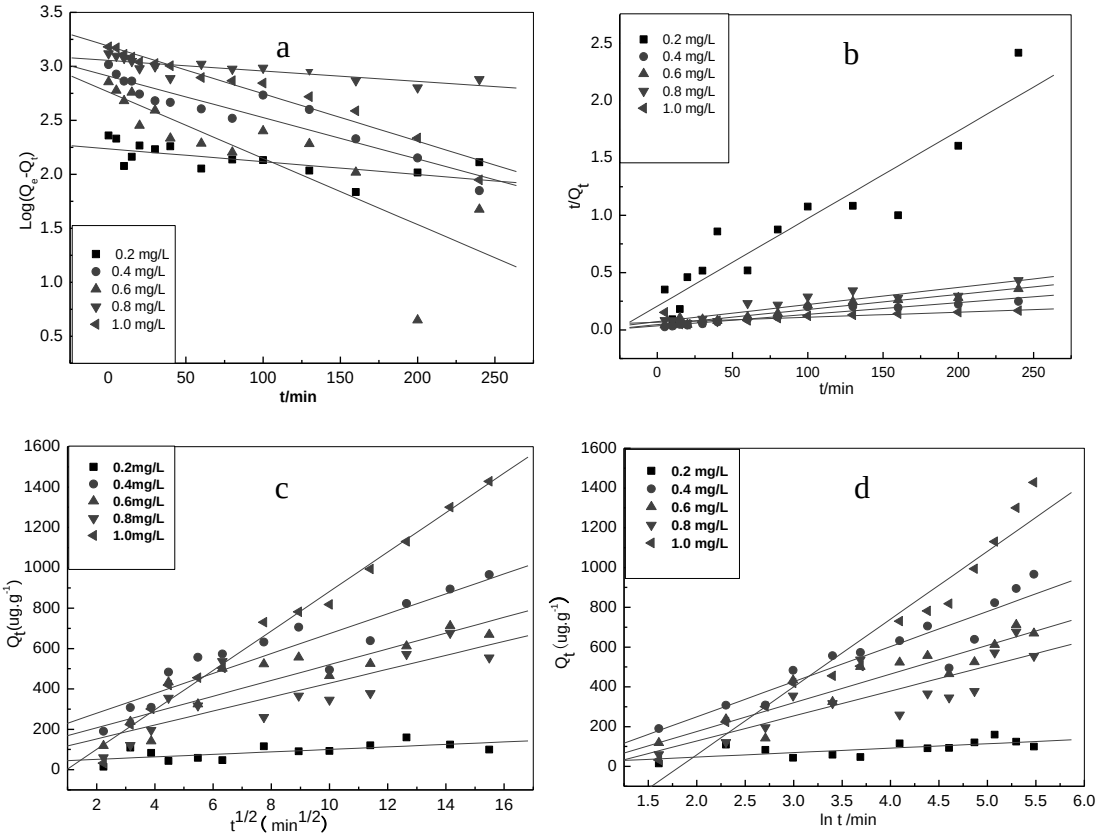

Fig. 5. Plots of the (a) pseudo-first order equation, (b) pseudo-second order equation, (c) intra-particle diffusion equation, and (d) Elovich equation for the adsorption kinetics of Cr(VI) on LTNA at different initial concentrations

Figure 5(c) is the plot of Q_t to $t^{1/2}$ at different initial Cr(VI) concentrations. If the curve passes through the origin (0, 0), then intra-particle diffusion can be considered the rate-limiting step, otherwise, the adsorption process is jointly controlled by a variety of adsorption mechanisms. However, the results of fitting did not pass through the origin (0, 0), indicating that particle diffusion is not the only rate-limiting step in the adsorption process (Acharya *et al.* 2009). The coefficients and numerical values from the equation are listed in Table 3. As the initial Cr(VI) concentration increased, the R^2 value also gradually increased, which is probably due to the porous structure of the LTNA, so that high Cr(VI) concentrations can lead to diffusion among the particles. Therefore, for high

Cr(VI) concentrations, the adsorption process proceeded with stronger intra-particle diffusion (Acharya *et al.* 2009).

The Elovich equation (Huang *et al.* 2012) is as follows,

$$Q_t = \frac{1}{\beta}\ln(\alpha\beta) + \frac{1}{\beta}\ln t \quad (6)$$

where α is the initial adsorption constant (mg g^{-1} min^{-1}) and β is a coefficient related to the surface coverage and the activation energy for chemical adsorption (g mg^{-1}).

Figure 5(d) shows the linear fit of the Elovich equation model when the LTNA resin adsorbs different concentrations of Cr(VI).

The best-fit values and coefficient of determination values for the Elovich equation are given in Table 3. It was found that at equilibrium, the Cr(VI) adsorption capacity of the LTNA resin gradually increased with an increase in Cr(VI) concentration. The corresponding coefficient of determination values for the Elovich equation also showed a gradually increasing trend, from 0.687 for a Cr(VI) concentration of 0.2 mg/L, to 0.973 when the Cr(VI) concentration was 1.0 mg/L. Thus, for higher initial Cr(VI) concentrations, the chemical activation energy was higher and there was more chemical adsorption, resulting in a trend of gradually increasing values for Q. These results indicate that the adsorption of Cr(VI) onto LTNA at higher concentrations is more consistent with the Elovich equation (Ho and Ofomaja 2005).

Table 3. Kinetic Parameters for the Adsorption of LTNA at Different Initial Cr(VI) Concentrations (at 298 ± 2 K)

Kinetics	Parameters	Cr^{6+} C_0 (mg/L)				
		0.2	0.4	0.6	0.8	1.0
Pseudo-first order	Qe,exp (μg/g)	228.53	716.68	1036.55	1311.91	1517.12
	K_1 (min^{-1})	0.00274	0.01412	0.00884	0.00230	0.01013
	Qe,cal (μg/g)	130.719	757.576	980.392	671.1401	2500
	R^2	0.65798	0.83739	0.93951	0.81208	0.97662
Pseudo-second order	K_2 (min^{-1})	0.00028	0.00038	0.000030	0.000031	0.0000024
	R^2	0.93574	0.97519	0.95308	0.92051	0.97249
Intra-particle diffusion	K_{int} (μg/g·$min^{1/2}$)	38.8266	129.339	181.0962	83.392	94.597
	R^2	0.67534	0.89404	0.92322	0.82167	0.99428
Elovich	α (μg/g·min)	24.5995	65.69891	98.02657	47.02429	54.96619
	β (μg/min)	0.044637	0.0069167	0.005658	0.007960	0.002933
	R^2	0.68737	0.92771	0.92892	0.83893	0.97337

Thermodynamic Studies

Thermodynamic considerations are necessary to conclude whether the adsorption process is spontaneous or not. The experimental data obtained at different temperatures were used to calculate the thermodynamic parameters such as Gibbs free energy ΔG^o (kJ mol^{-1}), enthalpy ΔH^o (kJ mol^{-1}), and entropy ΔS^o (kJ mol^{-1} K^{-1}). The Gibbs free energy change of the adsorption reaction (Fan *et al.* 2008) is given as follows,

$$\Delta G^{o} = -RT \ln K_L \quad (7)$$

$$\Delta G^{o} = \Delta H^{o} - T\Delta S^{o} \quad (8)$$

where K_L (L mg^{-1}) is the Langmuir equilibrium constant obtained from the plot of C_e/q_e *vs.* C_e, R is the ideal gas constant (8.314 J mol^{-1} K^{-1}), and T is the temperature in Kelvin (K). ΔH^{o} and ΔS^{o} can be calculated from the slope and the intercept of the plot of Gibbs free energy change, ΔG^{o}. The calculated results are shown in Table 4.

The positive ΔH^{o} value reveals that the adsorption process was endothermic, which also indicates that there was an interaction between the adsorbent and adsorbate. The negative values of ΔG^{o} confirm that the adsorption reaction was a spontaneous process with a high preference for Cr(VI) onto LTNA, which means that the adsorptive force was strong enough to break the potential and lead the reaction to bind Cr(VI) onto the surface functional groups of LTNA. The positive ΔS^{o} value shows an increasing trend of system to equilibrium and may suggest some changes on the interface structure of the adsorbent during the adsorption process.

Table 4. Thermodynamic Parameters for the Adsorption of Cr(VI) on LTNA at Different Temperatures*

Temperature (°C)	K_L (L/mg)	ΔG^{o} (kJ/mol)	ΔH^{o} (kJ/mol)	ΔS^{o} kJ/(mol K)	R^2
20	1.310	-0.657	12.7	0.046	0.998
30	1.563	-1.123			
40	1.828	-1.569			

*Adsorbent dose: 0.2 g, initial concentration: 0.8 mg/L, and contact time: 60 min

Desorption Studies

The Cr(VI) loaded adsorbents may lead to an environmental disposal issue because they are hazardous in nature if desorption and leaching occurs. Cr(VI) desorption from the adsorbent will solve this problem to some extent. The desorption percentage of Cr(VI) was determined in 0.1 M NaOH, 0.1 M EDTA, and 0.1 M HCl, respectively. It was observed that 89.16% of the loaded Cr(VI) stripped in 0.1 M NaOH, 68.83% stripped with 0.1 M EDTA, and 14.98% stripped with 0.1 M HCl in the first cycle. The presence of mainly Cr(VI) in the stripping solution during desorption studies showed the electrostatic interaction between Cr(VI) ions and LTNA. An alkaline medium would weaken the electrostatic interaction between the Cr(VI) ions and LTNA, promoting desorption. However, complete desorption was impossible, because the involvement of non-electrostatic forces between the Cr(VI) ions and LTNA (Singh *et al.* 2007).

CONCLUSIONS

1. In order to prompt the removal efficiency of larch tannin, LTNA resin was prepared under microwave irradiation.
2. The adsorption of Cr(VI) on LTNA was pH-dependent, the optimum adsorption was observed at pH 1.0, and the maximum adsorption capacity was 9.1 mg/g. Low pH rendered the LTNA surface more positively charged and increased the removal of

Cr(VI) in the aqueous phase, given that the binding of anionic Cr(VI) ion species with positively charged groups was enhanced.

3. The kinetic studies on the adsorption of Cr(VI) onto LTNA revealed that the experimental data fit the pseudo-second-order kinetic model and that film diffusion initially controls the adsorption process.
4. The dependence of Cr(VI) adsorption on temperature was investigated and the thermodynamic parameters ΔG^{o}, ΔH^{o}, and ΔS^{o} were calculated. The results showed a spontaneous and exothermic interaction process.
5. Ion exchange, electrostatic interactions, and complexation could be the possible mechanisms for the removal of heavy metal ions by LTNA.
6. The adsorption-desorption results demonstrated the practical application ability of LTNA for the removal of Cr(VI) from water and wastewater.

ACKNOWLEDGMENTS

This work was supported financially by the National Natural Science Foundation of China (Grant No. 31000277) and the Ph.D. Programs of Foundation of the Ministry of Education of China (Grant No. 20100062120005). We also wish to express our thanks for the Technical Research Project of Heilongjiang Provincial Education Department of China (Grant No. 12523016).

REFERENCES CITED

Acharya, J., Sahu, J. N., Mohanty, C. R., and Meikap, B. C. (2009). "Removal of lead(II) from wastewater by activated carbon developed from Tamarind wood by zinc chloride activation," *Chem. Eng. J.* 149(1-3), 249-262.

Ahalya, N., Kanamadi, R. D., and Ramachandra, T. V. (2005). "Biosorption of chromium (VI) from aqueous solutions by the husk of Bengal gram (*Cicer arientinum*)," *Electron. J. Biotechnol*. 8(3), 258-264.

Albadarin, A. B., Mangwandi, C., Al-Muhtaseb, A. H., Walker, G. M., Allen, S. J., and Ahmad, M. N. M. (2012). "Kinetic and thermodynamics of chromium ions adsorption onto low-cost dolomite adsorbent," *Chem. Eng. J.* 179, 193-202.

Anandkumar, J., and Mandal, B. (2009). "Removal of Cr(VI) from aqueous solution using Bael fruit (*Aegle marmelos correa*) shell as an adsorbent," *J. Hazard. Mater*. 168(2-3), 633-640.

Ayhan Şengil, I., and Özacar, M. (2009). "Competitive biosorption of Pb^{2+}, Cu^{2+} and Zn^{2+} ions from aqueous solutions onto valonia tannin resin," *J. Hazard. Mater*. 166(2-3), 1488-1494.

Aydın, Y. A., and Aksoy, N. D. (2009). "Adsorption of chromium on chitosan: Optimization, kinetics and thermodynamics," *Chem. Eng. J*. 151(1-3), 188-194.

Aoyama, M., and Tsuda, M. (2001). "Removal of Cr(VI) from aqueous solution by larch bark," *Wood Sci. Technol.* 35, 425-434.

Benhammou, A., Yaacoubi, A., Nibou, L., and Tanouti, B. (2007). "Chromium(VI) adsorption from aqueous solution onto Moroccan Al-pillared and cationic surfactant stevensite," *J. Hazard. Mater*. 140(1-2), 104-109.

Chand, R., Narimura, K., Hidetaka Kawakita, H., Ohto, K., Watari, T., and Inoue, K. (2009). "Grape waste as a biosorbent for removing Cr(VI) from aqueous solution," *J. Hazard. Mater*. 163(1), 245-250.

Fan, T., Liu, Y. G., Feng, B. Y., Zeng, G. M., Yang, C. P., Zhou, M., Zhou, H. Z., Tan, Z. F., and Wang, X. (2008). "Biosorption of cadmium(II), zinc(II) and lead(II) by *Penicillium simplicissimum*: Isotherms, kinetics and thermodynamics," *J. Hazard. Mater*. 160(2-3), 655-661.

Freundlich, H. M. F. (1906). "Over the adsorption in solution," *J. Phys. Chem.* 57, 385-471.

Guo, Y. P., Yang, S. F., Yu, K. F., Wang, Z. C., and Xu, H. D. (2002). "Adsorption of Cr(VI) on micro- and mesoporous rice husk-based active carbon," *Mater. Chem. Phys*. 78(1), 132-137.

Gupta, S., and Babu, B. V. (2009). "Removal of toxic metal Cr(VI) from aqueous solutions using sawdust as adsorbent: Equilibrium, kinetics and regeneration studies," *Chem. Eng. J*. 150(2-3), 352-365.

Gupta, V. K., Shrivastava, A. K., and Jain, N. (2001). "Biosorption of chromium(VI) from aqueous solutions by green algae *Spirogyra* species," *Water Res*. 35(17), 4079-4085.

Ho, Y. S., and Ofomaja, A. E. (2005). "Kinetics and thermodynamics of lead ion sorption on palm kernel fibre from aqueous solution," *Process Biochem*. 40(11), 3455-3461.

Homagai, P. L., Ghimire, K. N., and Inoue, K. (2010). "Adsorption behavior of heavy metals onto chemically modified sugarcane bagasse," *Bioresour. Technol*. 101(6), 2067-2069.

Hu, X. J., Wang, J. S., Liu, Y. G., Li, X., Zeng, G. M., Bao, Z. L., Zeng, X. X., Chen, A. W., and Long, F. (2011). "Adsorption of chromium (VI) by ethylenediamine-modified cross-linked magnetic chitosan resin: Isotherms, kinetics and thermodynamics," *J. Hazard. Mater*. 185(1), 306-314.

Huang, X., Liao, X. P., and Shi, B. (2010). "Tannin-immobilized mesoporous silica bead (BT-SiO_2) as an effective adsorbent of Cr(III) in aqueous solutions," *J. Hazard. Mater.* 173(1-3), 33-39.

Huang, Z. H., Liu, S. X., Zhang, B., Xu, L. L., and Hu, X. F. (2012). "Equilibrium and kinetics studies on the adsorption of Cu(II) from the aqueous phase using a β-cyclodextrin-based adsorbent," *Carbohydr. Polym*. 88(2), 609-617.

Karthikeyan, T., Rajgopal, S., and Miranda, L. R. (2005). "Chromium (VI) adsorption from aqueous solution by *Hevea brasilinesis* sawdust activated carbon," *J. Hazard. Mater*. 124(1-3), 192-199.

Kim, S., and Kim, H. J. (2003). "Curing behavior and viscoelastic properties of pine and wattle tannin-based adhesives studied by dynamic mechanical thermal analysis and FT-IR-ATR spectroscopy," *J. Adhesion Sci. Technol*. 17(10), 1369-1383.

Langmuir, I. (1918). "The adsorption of gases on plane surfaces of glass, mica and Platinum," *J. Am. Chem. Soc.* 40, 1361-1403.

Liu, S. X., Sun, J., and Huang, Z. H. (2010a). "Carbon spheres/activated carbon composite materials with high Cr(VI) adsorption capacity prepared by a hydrothermal method," *J. Hazard. Mater*. 173(1-3), 377-383.

Liu, W. F., Zhang, J., Zhang, C. L., Wang, Y. F., and Li, Y. (2010b). "Adsorptive removal of Cr (VI) by Fe-modified activated carbon prepared from *Trapa natans* husk," *Chem. Eng. J.* 162(2), 677-684.

Marjanović, V., Lazarević, S., Janković-Častvan, I., Potkonjak, B., Janaćković, Đ., and Petrović, R. (2011). "Chromium(VI) removal from aqueous solutions using mercaptosilane functionalized sepiolites," *Chem. Eng. J*. 166(1), 198-206.

Miretzky, P., and Cirelli, A, F. (2010). "Cr(VI) and Cr(III) removal from aqueous solution by raw and modified lignocellulosic materials: A review," *J. Hazard. Mater.* 180(1-3), 1-19.

Mitra, P., Sarkar, D., Chakrabarti, S., and Dutta, B. K. (2011). "Reduction of hexa-valent chromium with zero-valent iron: Batch kinetic studies and rate model," *Chem. Eng. J.* 171(1), 54-60.

Nakajima, A., and Baba, Y. (2004). "Mechanism of hexavalent chromium adsorption by persimmon tannin gel," *Wat. Res.* 38(12), 2859-2864.

Nakano, Y., Takeshita, K., and Tsutsumi, T. (2001). "Adsorption mechanism of hexavalent chromium by redox within condensed-tannin gel," *Wat. Res*. 35(2), 496-500.

Oo, C. W., Kassim, M. J., and Pizzi, A. (2009). "Characterization and performance of *Rhizophora apiculata* mangrove polyflavonoid tannins in the adsorption of copper (II) and lead (II)," *Ind. Crops and Prod*. 30(1), 152-161.

Owlad, M., Aroua, M. K., and Wan Daud, W. M. A. (2010). "Hexavalent chromium adsorption on impregnated palm shell activated carbon with polyethyleneimine," *Bioresour. Technol*. 101(14), 5098-5103.

Sankararamakrishnan, N., Dixit, A., Lyengar, L., and Sanghi, R. (2006). "Removal of hexavalent chromium using a novel cross linked xanthated chitosan agent," *Bioresour. Technol*. 97(18), 2377-2382.

Singh, V., Tiwari, S., Sharma, A. K., and Sanghi, R. (2007). "Removal of lead from aqueous solutions using *Cassia grandis* seed gum-graft-poly(methylmethacrylate)," *J. Colloid Interface Sci.* 316(2), 224-232.

Singha, B., and Kumar Das, S. (2011). "Biosorption of Cr(VI) ions from aqueous solutions: Kinetics, equilibrium, thermodynamics and desorption studies," *Colloids and Surf. B: Biointerfaces* 84(1), 221-232.

Tazrouti, N., and Amrani, M. (2009). "Chromium (VI) adsorption onto activated kraft lignin produced from alfa grass *(Stipa tenacissima)*," *BioResources* 4(2), 740-755.

Uysal, M., and Ar, I. (2007). "Removal of Cr(VI) from industrial wastewaters by adsorption Part I: Determination of optimum conditions," *J. Hazard. Mater*. 149(2), 482-491.

Wang, X. S., Li, Z. Z., and Tao, S. R. (2009). "Removal of chromium (VI) from aqueous solution using walnut hull," *J. Environ. Manage*. 90(2), 721-729.

Article submitted: December 5, 2012; Peer review completed: March 3, 2013; Revised version received: June 28, 2013; Accepted: July 12, 2013; Published: July 22, 2013.